

Evaluation of Non-Conforming Corroded Bridge Piers Exposed to Seismic Loads

Mohamed Husain, HebaA. Mohamed, Sayed Ahmed

Department of Structural Engineering, faculty of engineering, Zagazig University, Zagazig, Egypt

Abstract—Corrosion of steel reinforcement has been recognized as a major deterioration issue for the performance and safety of reinforced concrete bridge Piers. Reinforced concrete bridge piers with insufficient transverse reinforcement and non-seismic reinforcement details are vulnerable to shear failure and loss of axial load carrying capacity. In this paper, the behavior of corroded bridge piers non –conforming under seismic loading was numerically studied. The nonlinear 3-D finite-element model has been planned and implement on ANSYS platform and studied under cyclic lateral loads and different a range of axial force. The proposed FE model was verified with the experimental results of seven reinforced concrete bridge piers in three different experimental studies. Parametric study have been carried out to assess the effect of structure parameters such as the level of axial force, corrosion level , transverse reinforcement ratio and compressive strength of concrete on the lateral strength of corroded concrete bridge piers .

Index Terms—Bridge piers, Corrosion, non –conforming, FE, deterioration.

I. INTRODUCTION

Corrosion of steel reinforcement has been considered as a main major of deterioration for reinforced concrete (RC) structures. On the material level, due to volume change of corroded steel a bursting force arises on concrete causing concrete cover spalling as well as reduction in concrete bond, [1]. For the corroded reinforcement, some experimental studies decided that the cross-sectional area, strength and ultimate strain of steel reinforcement are significantly decreased due to corrosion [2, 3]. As a result, deterioration of mechanical properties of reinforcement and concrete adversely affect the long-term performance and safety of RC structures. Previous research mainly focuses on the causes and mechanism of reinforcement corrosion and its influences on the deteriorations of reinforcement and concrete [4,5]. To the best of the author’s knowledge, the subject of the behavior of corroded Rc bridge piers is not fully studied and there is a need for more research for it. Recently, several experimental investigations on the seismic behavior of corroded RC columns have been carried out in literature [6-9], which revealed that the corrosion phenomenon strongly affects the global performance of these structures, particularly their strength and ultimate drift capacity. So, it is important to conclude the effect of corrosion on major parameters of lateral resistance such as pier aspect ratio, concrete strength, axial

force ratio and longitudinal and transverse reinforcement ratio. Post-earthquake reconnaissance and experimental research indicate that existing building columns with light and inadequately detailed transverse reinforcement are vulnerable to shear failure during earthquakes. Shear failure can lead to reduction in building lateral strength, change in inelastic deformation mechanism, loss of axial load-carrying capacity, and ultimately, building collapse. Recognizing the risk posed by column shear failure, engineers evaluating existing buildings or designing new buildings for seismic effects aim explicitly to avoid column shear failure [10, 11]. The adoption of the 1976 Uniform Building Code (ICBO 1976), [12] resulted in important changes in the design and construction of reinforced concrete buildings in the seismically active western United States. The provisions of that code included new requirements for column shear strength and column transverse reinforcement detailing aimed at reducing the likelihood of column shear failure during earthquakes. Buildings constructed prior to the adoption of that code, as well as many more recent buildings constructed in regions of lower seismicity and not subject to the ductile design provisions of that code, may contain columns whose proportions and details do not meet the more stringent seismic design requirements of the 1976 Uniform Building Code and later codes. Such older existing building columns may be susceptible to failure with relatively low ductility. In this paper, the behavior of corroded bridge piers non –conforming under seismic loading was numerically studied. The nonlinear 3-D finite-element model has been planned and implement on ANSYS platform and studied under cyclic lateral loads and different a range of axial force. The proposed FE model was verified with the experimental results of seven reinforced concrete bridge piers in three different experimental studies. Parametric study have been carried out to assess the effect of structure parameters such as the level of axial force, corrosion level , transverse reinforcement ratio and compressive strength of concrete on the lateral strength of corroded concrete bridge piers.

II. RESEARCH SIGNIFICANT

Investigate the effect of various critical parameters on the behavior of corroded R.C bridge piers especially lateral load resistance. This paper presents FE model to evaluate the lateral load resistance of corroded bridge piers that not conforming to new design code taking into consideration all factors affecting on it. These models account for the

reduction in shear strength due to loss of bond between steel reinforcement and surrounding concrete and reduction in steel cross-sectional area and strength due to corrosion. In addition, these models take into account the effect of span to depth ratio, reinforcement ratio and concrete strength.

III. FE MODEL

A. Development of the model

The commercial FEA software ANSYS 17.2 was employed to perform this research.

B. Assumptions

Based on the available experimental data, the following assumptions were made: The corrosion is assumed to be uniform over the corroded reinforcement; the bond between steel reinforcement and surrounding concrete was simulated using an element taking into account bond deterioration under corrosion ; seismic loads was simulated using cyclic lateral displacement according to ACI 374.2R-13 [13]. The corrosion level of transverse reinforcement is slightly larger than that of the longitudinal reinforcement due to its smaller diameter and its distance to the outside environment is nearer, to simplify the analyses, the longitudinal reinforcement and transverse reinforcement are assumed to be corroded at the same level in the current parametric study.

C. Element types

As shown in Figure 1, the FE model contains four different types of elements: a 3-D SOLID65 element to model concrete elements, BEAM 188 element to model steel reinforcement, COMBIN39 spring element to model the bond between steel and surrounding concrete and SOLID 185 to simulate rigid Steel plate. The SOLID65 element is capable of crushing in compression and cracking in tension, and adopts a nonlinear behavior which makes it ideal for modeling concrete. The solid element is defined by eight nodes, each of which nodes has three degrees of freedom; translations in the nodal x, y, and z directions. The element allows the treatment of nonlinear material properties. The SOLID65 is capable of cracking (in three orthogonal directions), crushing, plastic deformation, and creep. The BEAM 188 element is a uniaxial tension-compression element capable of carrying tension and compression. This element is defined by two nodes with three degrees of freedom at each node: translations in the nodal x, y, and z directions. The element X-axis is oriented along the length of the element from node I toward node J. The element does not allow bending. In addition, plasticity, creep, rotation, large deflection, and large strain capabilities are considered. To consider sensitivity of the column behavior to the effects of several bond conditions, the spring element COMBIN39 of zero length was used to connect the nodes of the BEAM188 elements of the longitudinal reinforcement to SOLID65 element using the generalized force– deflection curves, i.e. bond-slip

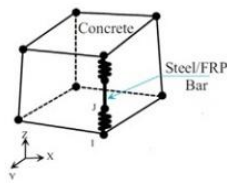
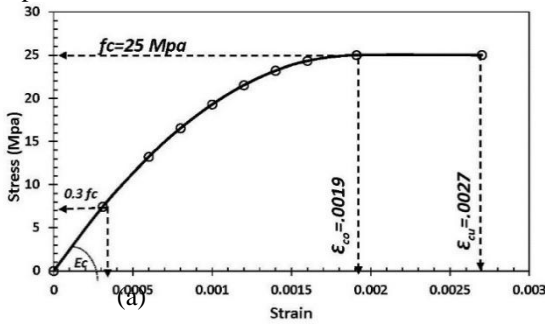
relationship. The concurrent nodes between the BEAM188 and SOLID65 were coupled in both the transverse and lateral directions. This element is a uni-directional element capable of determining the force-displacement nonlinearity equation. In addition, it has axial and torsional capability in one-, two and three-dimensional analyses. Its axial option, which is used here, has a maximum of three degrees of freedom in each node, [14].

IV. MATERIAL PROPERTIES AND REAL CONSTANTS

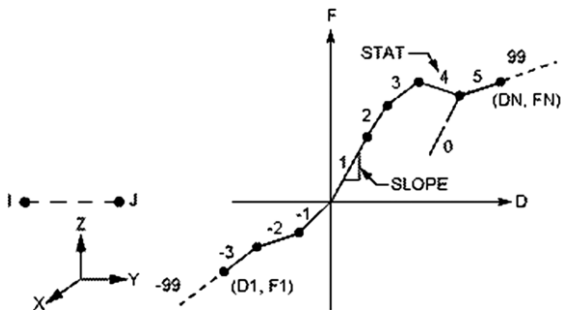
A. General

Several models for the stress-strain relation of concrete have been proposed, the modified Hognestad stress-strain relationship,[15] was adopted to define the multilinear isotropic concrete stress-strain curves and the model developed by Saatcioglu and Razvi,[16] was used for confined concrete required by ANSYS, as shown in Figure 2, the stress-strain curve plotted in Figure 2-a consists of typical stress- strain curve, the first point is defined as $0.30f_c$ and it represents the linear branch that satisfies Hook's law ,Wolanski , [17]. The next six points until (ϵ_{c0}) are calculated based on the equation describing the non-elastic branch of the modified Hognestad stress-strain relationship for un confined concrete or by using Saatcioglu and Razvi model for confined concrete as described below .The last two points represent the linear branch of the modified Hognestad stress-strain relationship. The linear branch of the curve was considered perfectly plastic since the latest versions of ANSYS, [14]do not tolerate negative slopes in stress-strain plots.It is important to note that the initial slope of stress-strain diagram is almost equal to the modulus of elasticity which is calculated based on the above-mentioned equations. Figure 2-b represent stress -strain curve for unconfined concrete with concrete compressive strength $(f_c=25 \text{ Mpa})$.The modulus of elasticity of concrete was $4,750 *(f_c)^{.5} \text{ (Mpa)}$, uniaxial cracking stress (modulus of rupture) was $0.62*(f_c)^{.5} \text{ (Mpa)}$ and Poisson's ratio was assumed to be 0.2. ANSYS assumes a linear stress-strain relationship for concrete in tension until the uniaxial cracking stress is reached as described in Figure 2-c.Shear transfer coefficients range from 0 to 1, with 0 representing smooth crack (complete loss of shear transfer) and 1.0 representing a rough crack (no loss of shear transfer),[14].Shear transfer coefficient for an open crack was considered to be 0.3, and the shear transfer coefficient for a closed crack was considered to be 0.90. The uniaxial cracking stress and the uniaxial crushing stress were assumed to be the modulus of rupture and the concrete compressive strength respectively. The biaxial crushing stress, hydrostatic pressure, hydro biaxial crush stress, hydrostatic stress, and tensile crack factor were set equal to zero, which is their default values determined by ANSYS,[14]. These values of the above coefficients were verified by a preliminary analysis

performed by the author to the best agreement with experimental data.

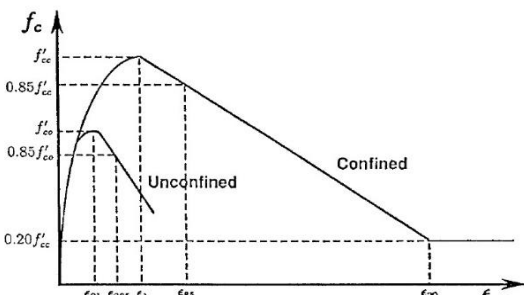


(b)

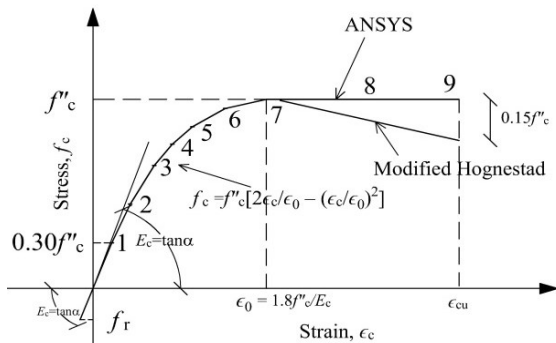


(c)

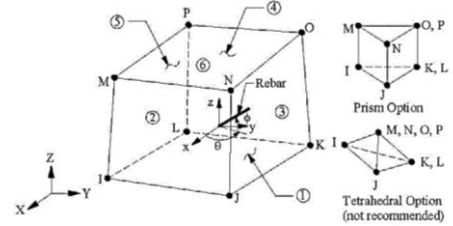
Fig 1: Geometry of: a- SOLID65; b- BEAM 188 and c- COMBIN39 element (ANSYS 17.20).



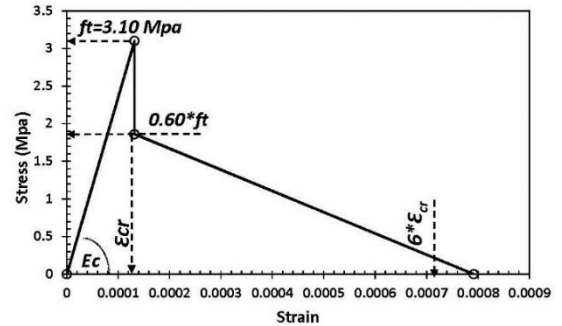
(a)



(b)



(c)



(d)

Fig 2: Stress-strain diagrams for concrete: (a) typical confined and un confined; (b) modified Hognestad for un confined and typical for ANSYS; (c) un confined concrete with compressive strength 25 Mpa and (d) tension model in ANSYS for f_c=25 Mpa.

B. Modeling of unconfined concrete cover

Corrosion transforms steel into rust, resulting in the volumetric expansion that can develop the splitting stresses in concrete. The cracking and spalling of concrete induced by these stresses can be modeled by reducing the strength of concrete elements belonging to this region, as follows [18]:

$$f'_{cc} = \frac{f'_c}{1+k \frac{\epsilon_1}{\epsilon_{co}}} \dots\dots\dots \text{Equation 1}$$

Where k is the coefficient with regard to the diameter and roughness of reinforcement, the value k = 0.1 proposed in [19] is adopted in this study; ϵ_1 is the smeared tensile strain, regarding to the crack width of concrete due to corrosion, which can be estimated as:

$$\epsilon_1 = \frac{\sum w_{cr}}{b_0} = \frac{\sum 2\pi (v_{cr}-1)x}{b_0} \dots\dots\dots \text{Equation 2}$$

$$x = \frac{(D_0 - D_c)}{b_0} \dots\dots\dots \text{Equation 3}$$

Where b_0 is the circumference of a RC pier section; w_{cr} is the crack width induced by corrosion of reinforcement; x is the depth of corrosion attack; v_{cr} is the ratio of the volumetric expansion of the corroded steel to the virgin steel that depends on the type of corrosion products. The value of $v_{cr} = 2$ recommended by [20]. According to the recommendation of Hanjari et al.,[21], because of the cracked concrete around corroded reinforcement induced by corrosion, the tensile concrete strength should be reduced proportionally to the reduction in compressive concrete strength as following expression:

$$f'_{tc} = \frac{f'_c}{f'_c} f'_t \dots\dots\dots \text{Equation 4}$$

Where the tensile strength f'_t of uncorroded concrete estimated based on the ACI 318-14, [22] as follows:

$$f'_t = 0.62 \sqrt{f'_c} \quad \dots\dots\dots \text{Equation 5}$$

C. Modeling of corroded reinforcement

Several researchers experimentally investigated the effect of corrosion on the mechanical properties and strength of steel reinforcement. They reported a decrease in the cross sectional area and strength of steel reinforcement embedded in concrete due to corrosion. Based on both the accelerated and simulated corrosion tests on bare bars and on bars embedded in concrete, Du et al. [23] suggested Eqs. (6-8) to estimate the residual cross-sectional area and strength of corroded reinforcing bars. These equations are based on a regression analyses performed on both sets of test data.

$$A_{S(corr)} = (1 - 0.01 Q_{corr}) A_S \quad \dots\dots\dots \text{Equation 6}$$

$$f_{y(corr)} = (1 - 0.005 Q_{corr}) f_y \quad \dots\dots\dots \text{Equation 7}$$

$$Q_{corr} = \left[\left(1 - \left(\frac{d_{0(corr)}}{d_0} \right)^2 \right) \right] \times 100 \quad \dots\dots\dots \text{Equation 8}$$

Where:

$A_{S(corr)}$; average cross-sectional area of corroded reinforcement, A_S ; initial cross-sectional area of non-corroded reinforcement, Q_{corr} ; corrosion degree, which is calculated as the mass loss (%), $f_{y(corr)}$ = yield strength of corroded bars, f_y = yield strength of non-corroded bars and $d_0, d_{0(corr)}$ are the diameters of the uncorroded and corroded reinforcing bars, respectively.

D. Modeling of confined concrete core

As mentioned above, the corrosion of confinement reinforcement results in the properties degradation of confined core concrete, particularly the maximum strength and the ultimate strain which can be estimated when the transverse confining reinforcement fractures. In this paper, the stress-strain relationship developed by Saatcioglu and Razvi, [16] is utilized and modified to simulate the behavior of confined concrete due to corrosion. According to this model, the confined strength and ultimate strain of concrete are estimated as:

$$f'_{cc} = f'_{co} + K \cdot f_{le} \quad \dots\dots\dots \text{Equation 9}$$

$$K = \frac{(K_1 \cdot f_{le})}{f_{co}} \quad \dots\dots\dots \text{Equation 10}$$

$$\epsilon_{uc} = 260 \cdot \rho \cdot \epsilon_l + \epsilon_{uc} \quad \dots\dots\dots \text{Equation 11}$$

$$\rho = \frac{\sum A_s}{b(b_{cx} + b_{cy})} \quad \dots\dots\dots \text{Equation 12}$$

Where:

f_c ; Stress in concrete (in MPa), f'_{cc} ; Confined concrete strength in member (in MPa), f'_{co} ; Unconfined concrete strength in member (in MPa), f_{le} ; Equivalent lateral pressure that produces the same effect as uniformly applied pressure, ρ ; Average lateral confinement pressure (in MPa), A_s ; Area of one leg of transverse reinforcement (in mm²), b_c ; Core dimension measured center-to-center of perimeter hoop (in mm), ϵ_l ; Strain corresponding to peak stress of confined concrete, ϵ_{85} ; Strain corresponding to 85 % of peak stress of confined concrete on the

descending branch, $\epsilon_{0.85}$; Strain corresponding to 85 % of peak stress of unconfined concrete on the descending branch, K, k_1 Coefficients; ρ ; Reinforcement ratio. b_{cx}, b_{cy} ; Core dimensions in x and y directions, respectively (in mm), for more details refer to Saatcioglu and Razvi, [16]. To take into consideration the corrosion effect, this coefficient can be calculated by reducing the average cross-sectional area and strength of both longitudinal and transverse reinforcing bars, as mentioned in Eqs. (6) and (7). Figure 3- presents the modeling of uncorroded and corroded confined concrete under compression.

E. Bond deterioration model

1) Bond strength of corroded reinforcement

Various bond strength deterioration models of corroded reinforcement induced by corrosion are available in literature [24, 25]. In this paper, the bond strength model developed by Maaddawy et al., [26] is utilized to calculate the maximum bond strength of corroded reinforcement. As compared to other empirical bond strength models, some advantages of this model include its ability to take into account the contributions from concrete and stirrup independently and also consider the effect of impressed current density for accelerated corrosion on the bond strength deterioration. In this model, the maximum bond stress of corroded reinforcement τ_{maxc} can be expressed as follows:

$$\tau_{maxc} = R \left(0.55 + 0.24 \left(\frac{C_c}{d_b} \right) \sqrt{f'_c} + 0.191 \frac{A_v + I_{yh}}{S d_b} \right) \dots \text{Equation 13}$$

$$R = (A_1 + A_2 X_{corr}) \dots \text{Equation 14}$$

and R is a factor that considers the reduction of the bond strength in which A_1 and A_2 are coefficients reflecting the rate of corrosion in an accelerated corrosion process. For corrosion process of $0.09 \mu A/cm^2$, the values of these coefficients were determined as $A_1 = 1.104, A_2 = -0.024$. Finally, X is the corrosion rate, which is stated as a percentage of the rebar mass loss. For more details see [26].

2) Modified local bond stress-slip model

To take consideration the influence of corrosion on the local bond behavior, the bond stress-slip model developed in the CEB-FIP, [24] is utilized and modified by using Eq. (13) as:

$$\begin{aligned} \tau &= \tau_{maxc} \left(\frac{s}{S_1} \right)^\alpha & 0 \leq s \leq S_1 \\ \tau &= \tau_{maxc} & S_1 \leq s \leq S_2 \\ \tau &= \tau_{maxc} - (\tau_{maxc} - \tau_f) \left(\frac{s - S_2}{S_3 - S_2} \right) & S_2 \leq s \leq S_3 \\ \tau &= \tau_f & S_3 < s \end{aligned} \dots \text{Equation 15}$$

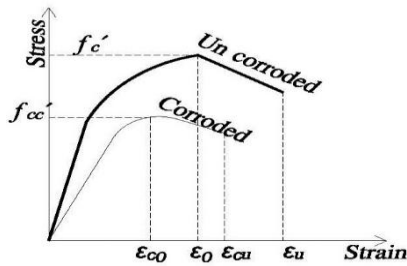
It is noted that with the generally designed cover concrete thickness and transverse reinforcement amount, the bond failure in corroded reinforcement is mostly due to splitting [25]. Therefore, the values of parameters of the modified bond stress-slip model can be chosen as: $\alpha = 0.40$; $S_1 = 0.6 \text{ mm}$; $S_2 = 0.6 \text{ mm}$; $S_3 = 2.50 \text{ mm}$; $\tau_f = 0.15 \tau_{maxc}$ Figure 3- shows an example of the modified bond model for uncorroded and corroded reinforcing bars.

V. RIGID PLATE

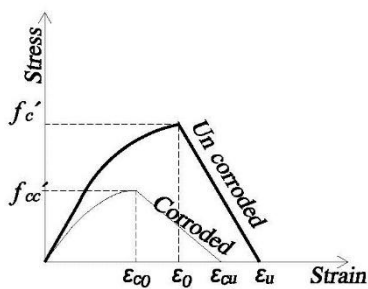
In order to avoid stress concentration at locations on which the loads are applied, a rigid steel plate is modeled using Steel plate elements (Solid185). Continuum element type with elastic property is used to model the rigid plate. A very high modulus of elasticity and 0.3 Poisson's ratio has assumed for the element to present a rigid plate transferring the loads to the reinforced concrete uniformly.

VI. BOUNDARY CONDITIONS AND LOADING

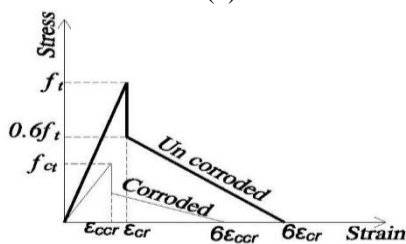
All the columns in this research, including experimental test columns studied by others and the current study's FE models are modeled as cantilevers (single or double) in ANSYS. Column bases are defined as fixed supports; then all degrees of freedom at all nodes of base elevation are restricted as shown at Figure 3-f. All the columns were tested under combined constant axial load and cyclic lateral displacement. The first step of analysis is applying axial load to the rigid plate at top of the column. Next step is applying cyclic lateral load; at which lateral displacement is applied to the rigid plate at side in x- direction. The cyclic loading history according to ACI 374.2R-13 [13] was used and is presented in Figure 4-e. The lateral displacement cycles were repeated twice with amplitudes of 0.5Δy, 1.0Δy, 2.0Δy, 3.0Δy, 4.0Δy, 5.0Δy, etc. until failure, where Δy is the yield displacement evaluated assuming effective stiffness of columns.



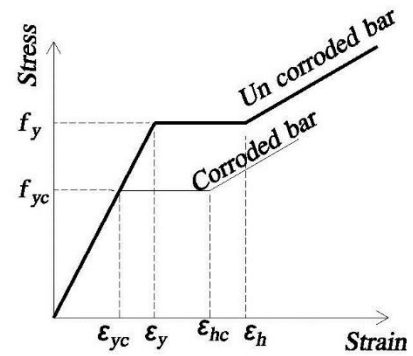
(a)



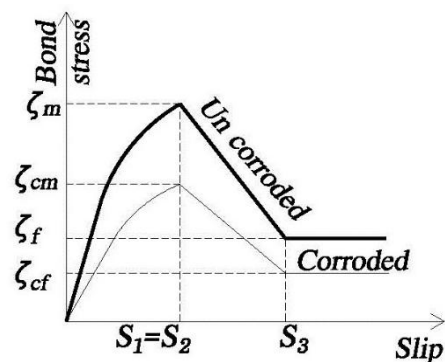
(b)



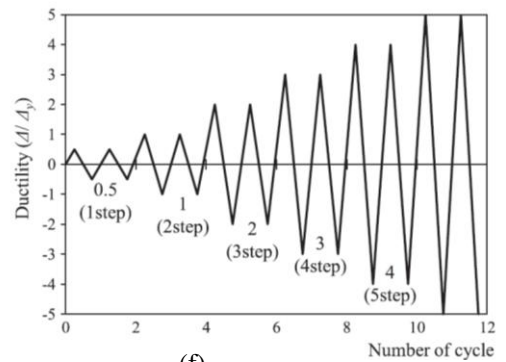
(c)



(d)



(e)



(f)

Fig 3: Pier FE model: (a) Core concrete in compression; (b) Cover concrete in compression; (c) Concrete in tension; (d) Steel rft. ; (e) Bond slip model and (f) lateral cyclic displacement.

VII. VALIDATION OF FINITE ELEMENT MODEL

Three experimental studies reported in literature [6, 7, and 8] on the performance of corroded RC columns under the simulated seismic loading are selected to validate the accuracy of the proposed FE model. The first experimental study conducted by Meda et al., [6] includes four RC columns with the same specifications in which the first two columns were accelerated corrosion, and then the reinforcement was extracted from these RC columns and tested in tension to study about the corrosion effect on the stress-strain relationships of corroded reinforcement. The third column was corroded up to a desired corrosion level of approximately 20% and subjected to cyclic loading while

the last column was used as reference un corroded specimen for comparison against the corroded RC column, it is noted that only longitudinal reinforcing bars were corroded. In the second experimental study carried out by Gong.,[7] comprised 14 RC columns owing the same specifications, which were subjected to different axial force ratios from 0.13 to 0.35 and varying corrosion levels. In this experimental program, both longitudinal and transverse reinforcing bars were corroded until the expected corrosion levels from 0 to 19.17% in terms of mass loss, he investigated the effect of combined CFRP and steel jacket retrofitting system on corroded RC columns. In the third experimental study carried out by Wang.,[8] comprised 17 RC columns owing the same specifications, which were subjected to different axial force ratios from 0 to 0.5 and varying corrosion levels. In this experimental program, both longitudinal and transverse reinforcing bars were corroded until the expected corrosion levels from 0 to 25% in terms of mass loss. In total, the experimental data of 7 RC columns in three experimental studies were selected to validate the proposed FE model, in which both uncorroded and corroded RC columns as well as various corrosion levels were examined. The details of these RC column specimens are shown in Table 1 and Figure 4 while their material properties used in the FE analyses are indicated in Table 2. Table 3 summarized the maximum lateral load resistance results from experimental and FE analysis. As observed, there is a good correlation in the overall global behavior between the experimental and FE results in terms of the initial stiffness, maximum lateral load resistance, and maximum displacement.

on the backbone curve of lateral load-displacement relationships in which the corrosion level with values 0%, 10 %, 20% and 40% was studied. As observed, the higher corrosion level results in the lower lateral load resistance and its significant reduction can be seen when the RC piers are highly corroded, that is the corrosion level from 20% to 40%. For example, the studied group (2), piers with the axial force ratio of 0.20 and transverse reinforcement ratio of 0.25%, when the corrosion level increases from 0% to 10%, 20%, and 40%, the lateral load resistance reduces 20%, 34%, and 48%, respectively. The more serious deterioration of lateral load resistance in the group (1) piers with axial force ratio of 0.3 and transverse reinforcement ratio of 0.17%, that is the decrease of 22%, 34%, and 43% can be seen with the rise of corrosion level from 0 to 10%, 20%, and 40%, respectively. Therefore, it is concluded that the corrosion effect on the lateral load resistance deterioration is more critical in cases of lower transverse reinforcement ratio, lower axial force ratio and higher corrosion level, as shown Figure 8.

VIII. PARAMETRIC INVESTIGATION

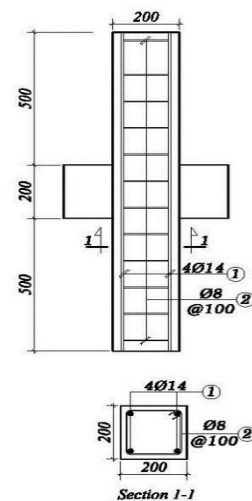
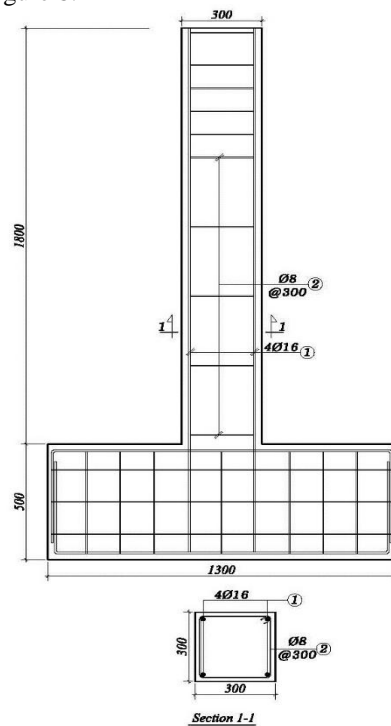
A. Numerical models of corroded RC columns

Adopting the proposed 3D non-linear FE model discussed above, numerical simulations were performed to study the influence of various parameters on the seismic behavior of corroded RC bridge piers, and to further estimate the reduction of their lateral load resistance. An extensive parametric study was carried out, including corrosion level, column aspect ratio, axial force ratio, transverse reinforcement ratio, and compressive concrete strength. Table 4 summarized the range of studied parameters. The parametric investigation is conducted by analyzing the FE models of 2 RC columns groups (1, 2), as indicated in Figure 5. The group (1, 2) are not meet the requirement design for seismic zones according to their requirement in the ACI 318-14 [22] with insufficient stirrups requirement in the plastic hinge zone. Figure 6 shows the load-displacement hysteretic curves of RC piers from FE.

B. Numerical results of corroded RC piers

1. Effect of corrosion level

The FE analyses for the constructed models subjected to different corrosion levels are presented in this section. Figure 7 demonstrates the effect of corrosion level



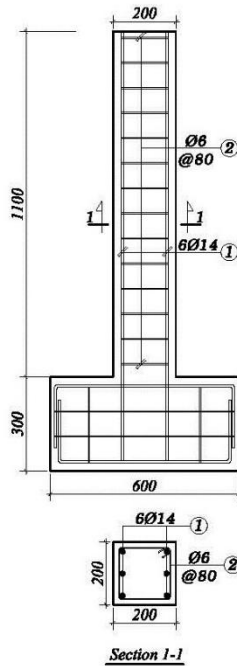


Fig 4: Details of specimens tested by: (a) Meda et al. [6]; (b) Gong’s [7] ; (c) Wang [8]

Table 1 Summary of RC column specimens to validate the proposed FE model.

Specimens	bxh (mm)	L (mm)	Aspect ratio (a/d)	Longitudinal RFT.	Transverse RFT.	Axial force ratio (P/(f _c A _g))	Corrosion level	Test type
UC [6]	300x300	1800	5.33	4Ø16 ρ _t =0.89 %	Ø8 @300 ρ _v =0.17%	0.22	0	Cantilever
CC [6]							20	
A0[7]	200x200	1200	2.5	4Ø14 ρ _t =1.53 %	Ø8 @100 ρ _v =0.5%	23.4	0	Double cantilever
B3[7]							16.8	
C2[7]							11.49	
ZZ-1[8]	200x200	1100	5.5	6Ø14 ρ _t =2.30 %	Ø6 @80 ρ _v =0.35%	0.34	0	Cantilever
Z-4[8]							18	

Table 2 Material properties of RC column specimens in FE analyses.

Specimens	Un-confined Cover Concrete		Confined Core Concrete		Longitudinal RFT.	Transverse RFT.	Max.Bond
	f _c (Mpa)	f _t (Mpa)	f _c (Mpa)	f _t (Mpa)	f _y (Mpa)	f _{yt} (Mpa)	ζ _{max} (Mpa)
UC [6]	20	2.77	21.83	2.9	520	520	5.18
CC [6]	10.62	1.47	21.58	2.88	468	520	2.81
A0[7]	44.8	4.15	48.67	4.33	384.77	326.95	9.37
B3[7]	22.79	2.11	48.23	4.31	352	299	5.6
C2[7]	27.14	2.51	48.37	4.31	363	308	6.72
ZZ-1[8]	24.56	3.07	28.17	3.29	415	325	6.42
Z-4[8]	9.6	1.2	27.74	3.27	378	296	3.42

Table 3 Comparisons of results

Specimens	Maximum lateral load (KN)	
	Experimental	F.E.A
UC [6]	63	63.5
CC [6]	46	46.45
A0[7]	190.87	190
B3[7]	173.2	168
C2[7]	167.8	146
ZZ-1[8]	51.57	48.6
Z-4[8]	41.9	42.7

Table 4 Parameters study

No.	Parameters	Notation	Range of study
1	Corrosion level	C.R (%)	0.0, 10.0 , 20.0 , 40.0
2	Compressive strength of concrete (Mpa)	f_c	25 , 50
3	Axial force ratio (N.R)	$N/(f_c A_g)$ (%)	10, 20, 30
4	Longitudinal reinforcement ratio (p_v)	$A_s/(b.h)$ (%)	2.01(10 ϕ 16) ,
5	Longitudinal reinforcement strength (Mpa)	F_v/f_u	400/600
6	Transverse reinforcement ratio (ρ_t)	$A_{v_t}/(b.s)$ (%)	0.17 (ϕ 8 @300 with 2 branshes), 0.25 (ϕ 8 @200 with 2 branshes),
7	Transverse reinforcement strength(Mpa)	F_v/f_u	280/450
8	Cross section (mm)	$b*h*L$	200*500*1500
9	Shear span to depth ratio	(L/d)	3.26

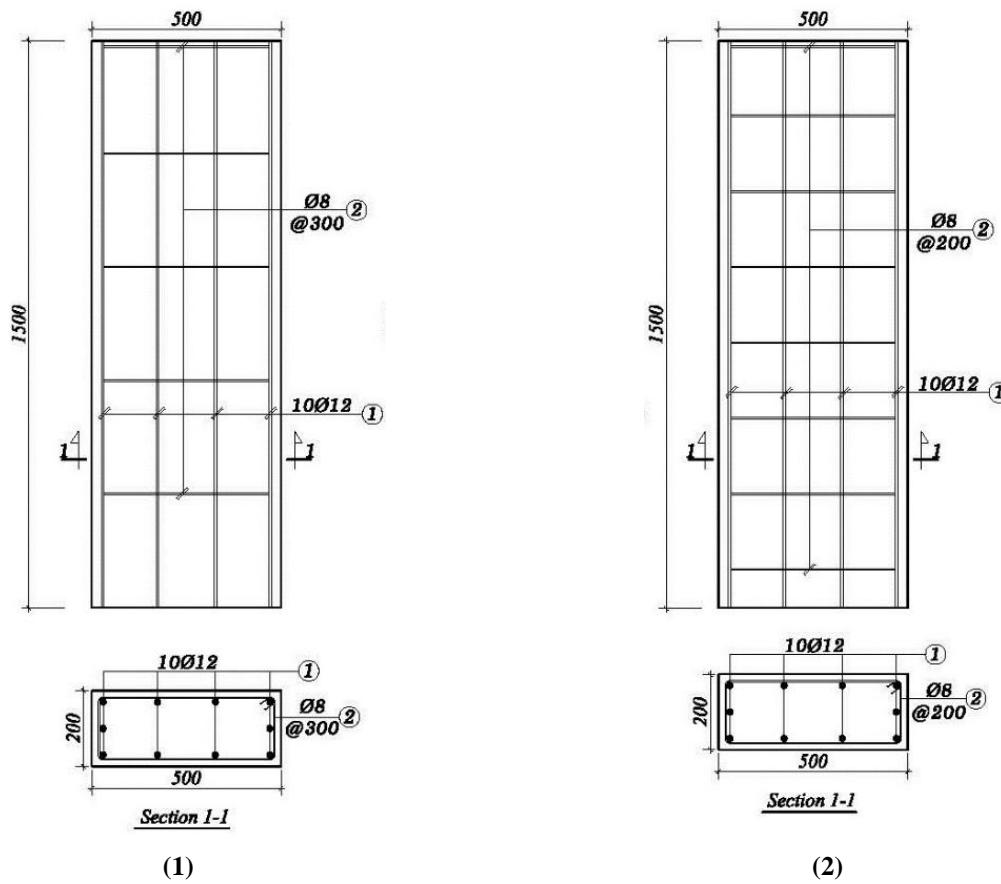


Fig 5: Details of study specimens 1-Group (1) 2-Group (2)

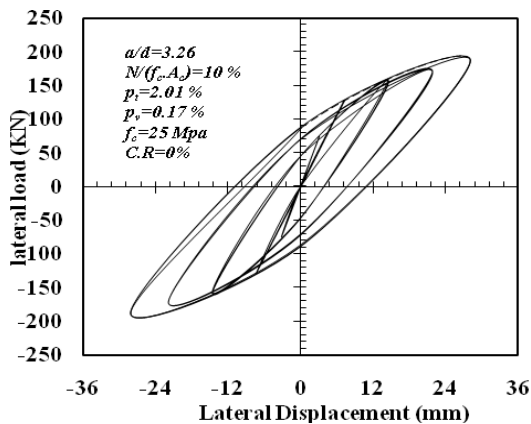


Fig 6: Load-displacement hysteretic curves of RC piers.

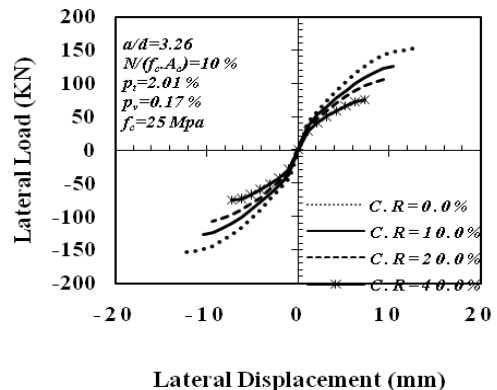


Fig 7: The backbone curve of corroded RC piers with different corrosion level.

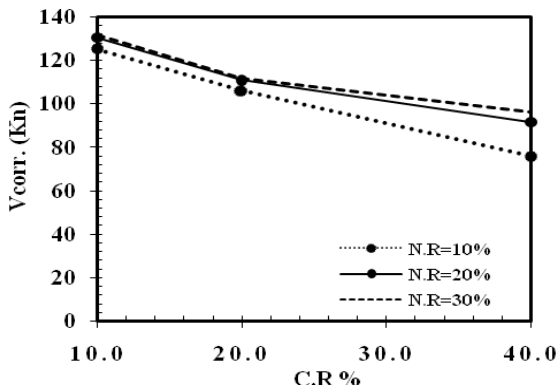


Fig 8: Effect of corrosion level on the backbone curve of corroded RC piers at $p_v=0.17\%$ and $f_c=25\text{Mpa}$.

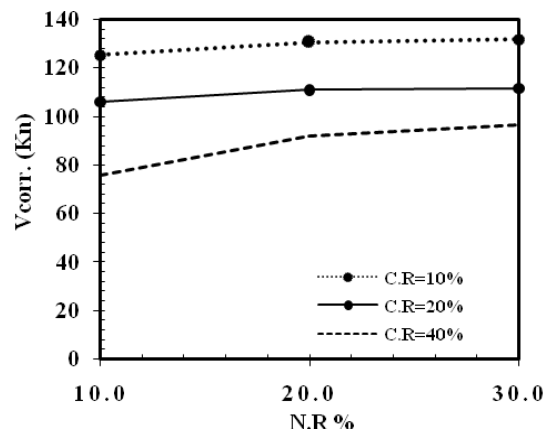


Fig 11: Effect of axial force ratio on the backbone curve of corroded RC piers at $p_v=0.17\%$ and $f_c=25\text{Mpa}$.

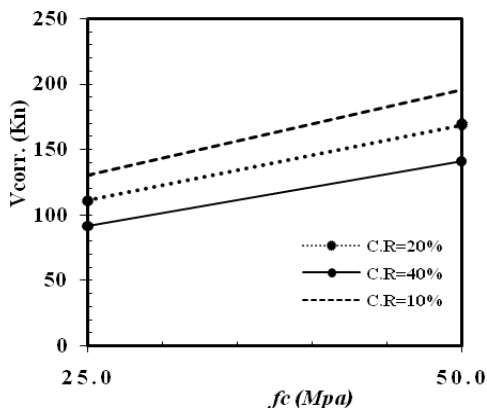


Fig 9: Effect of compressive strength on the backbone curve of corroded RC piers at $N.R=20\%$ and $p_v=0.17\%$

2. Effect of compressive concrete strength

The FE results showing that at the same corrosion level, the lateral load resistance of corroded RC piers increases with the increase of compressive concrete strength. For example, as shown in Figure 9 piers subjected to corrosion level of 40% and axial force ratio of 0.2, when the compressive concrete strength increases from 25 MPa to 50MPa, the lateral load resistance rises by approximately 54%. It is noted that the increase of compressive strength have significant effect on the lateral load resistance of corroded bridge piers with high corrosion level more than those with low corrosion level.

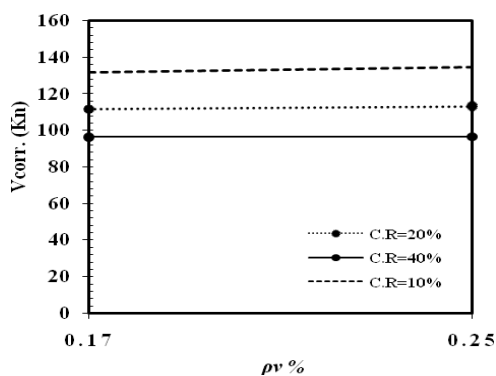


Fig 10: Effect of transverse reinforcement ratio on the backbone curve of corroded RC piers at $N.R=30\%$ and $f_c=25\text{Mpa}$.

3. Effect of transverse reinforcement ratio

Figure 10 shows the effect of stirrups amount on the performance of corroded RC piers. Piers subjected to the axial force ratio of 0.3, and corrosion level 10 % an approximately 3% increase of lateral load resistance when transverse reinforcement ratio increase from 0.17% to 0.25%. It is noted that the Effect of transverse reinforcement ratio is clear on piers with low corrosion level than those with high corrosion level.

4. Effect of axial force ratio

The axial force ratio with values 0.1, 0.20 and 0.3 was investigated. Figure 11 indicates that the lateral load resistance of corroded piers rises with an increase in axial force especially with high corrosion level, for example, the corroded piers in group (1) subjected to the corrosion level of 10 %, the lateral load resistance rises by approximately 4% and 1% when the axial force increases from 0.1 to 0.2, and 0.3, respectively, and for the same group at corrosion level 40% the lateral load resistance rises by approximately 21% and 5% when the axial force increases from 0.1 to 0.2, and 0.3, respectively. It is noted that the axial force ratio increase lateral load resistance at high corrosion level than piers with low corrosion level.

IX. CONCLUSIONS

The effect of reinforcement corrosion on the seismic behavior of non-conforming RC piers are numerically studied with 3D non-linear FE ANSYS software. The main structural parameters affecting on the lateral strength of corroded RC bridge piers such as corrosion level, transverse reinforcement ratio, axial force ratio and concrete compressive strength are studied. Based on the finite element analysis and dissections of results, conclusions can be summarized:

1. There is a good correlation in the overall global behavior between the experimental and FE results in terms of the initial stiffness, maximum lateral load resistance, and maximum displacement. The constructed finite element model can be used for analyzing any corroded bridge

piers under seismic loads with the consideration of degradation of corroded materials.

2. The lateral resistance of corroded RC piers decrease when the increase of corrosion level. The deterioration is more significant in RC piers subjected to higher corrosion levels (20–40%) than those under low corrosion levels (0–10%). The results concluded that the corrosion effect is more critical in cases of lower transverse reinforcement ratio and lower axial force ratio.
3. The increase of compressive strength has significant effect on the lateral load resistance of corroded bridge piers with high corrosion level more than those with low corrosion level.
4. The Effect of transverse reinforcement ratio is clear on piers with low corrosion level than those with high corrosion level.
5. The axial force ratio increase lateral load resistance at high corrosion level than piers with low corrosion level.

X. LIMITATIONS AND RECOMMENDATIONS FOR FUTURE STUDY

- 1- The FEA models and the proposed practical model can be used by engineers in practice to estimate the lateral capacity of severely corroded RC columns.
- 2- Further studies are necessary to provide a practical model for estimating the lateral capacity of severely corroded RC columns that fail in flexure.
- 3- For additional verification of the developed models and due to the limited availability of experimental data, it is recommended that further experiments be performed.

REFERENCES

[1] Y.-C. Ou, H.-D. Fan, N.D. Nguyen, “Long-term seismic performance of reinforced concrete bridges under steel reinforcement corrosion due to chloride attack”, *Earthquake Eng. Struct. Dynam.* 42 (2013) 2113–2127.

[2] Y.G. Du, L.A. Clark, A.H.C. Chan, “Residual capacity of corroded reinforcing bars”, *Mag. Concr. Res.* 57 (2005) 135-147.

[3] M.G. Stewart, “Mechanical behavior of pitting corrosion of flexural and shear reinforcement and its effect on structural reliability of corroding RC beams”, *Struct. Saf.* 31(2009)19-30.

[4] J. Cairns, G.A. Plizzari, Y. Du, D.W. Law, C. Franzoni, “Mechanical properties of corrosion-damaged reinforcement”, *Mater. J.* (2005) 102.

[5] H.-S. Lee, S.-H. Cho, “Evaluation of the mechanical properties of steel reinforcement embedded in concrete specimen as a function of the degree of reinforcement corrosion”, *Int. J. Fract.* 157 (2009) 81–88.

[6] A. Meda, S. Mostosi, Z. Rinaldi, P. Riva, “Experimental evaluation of the corrosion influence on the cyclic behavior of RC columns”, *Eng. Struct.* 76 (2014) 112–123.

[7] Li J, Gong J, Wang L. “Seismic Behavior of Corrosion-damaged Reinforced Concrete Columns Strengthen Using Combined Carbon Fiber-reinforced Polymer and Steel Jacket”, 2009, *Journal of Construction and Building Materials*, No. 23, pp. 2653-2663.

[8] X. Wang, “Research of Seismic Performance and Hysteretic Mode of Corroded Reinforced Concrete Members Master, Xi’an.

[9] C. Goksu, “Seismic Behavior of RC Columns with Corroded Plain and Deformed Reinforcing Bars” Phd, Istanbul Technical University, Turkey, 2012.

[10] American Concrete Institute (ACI). (2002). “Building code requirements for structural concrete.” ACI Committee 318, Farmington Hills, Mich.

[11] Federal Emergency Management Agency (FEMA). (1997). “NEHRP guidelines for the seismic rehabilitation of buildings.” FEMA 273, Washington, D.C.

[12] International Conference of Building Officials (ICBO). (1976). *Uniform Building Code*, Whittier, Calif.

[13] ACI 374.2R-13. “Guide for Testing Reinforced Concrete Structural Elements Under Slowly Applied Simulated Seismic Loads”. ACI Committee 374; 2013.

[14] ANSYS User’s Manual, Release 17.0. ANSYS, INC., Canonsburg, Pennsylvania; 2017.

[15] Hognestad, E. “A study on combined bending and axial load in reinforced concrete members”. Univ. of Illinois Engineering Experiment Station, Univ. of Illinois at Urbana-Champaign, IL, 1951, 43-46.

[16] Salim Razvi and Murat Saatcioglu., “Strength and Ductility of Confined Concrete”, *Journal of Structural Engineering*, Volume 118 Issue 6 - June 1992.

[17] Wolanski, A.J., “Flexural behavior of reinforced and prestressed concrete beams using finite element analysis”, M.S. Thesis, Marquette University, Wisconsin, 2004.

[18] D. Coronelli, P. Gambarova, Structural assessment of corroded reinforced concrete beams: modeling guidelines, *J. Struct. Eng.* 130 (2004) 1214–1224.

[19] M. Cape, Residual service-life assessment of existing R/C structures (MS thesis), Chalmers Univ. of Technology, Goteborg (Sweden) and Milan Univ. of Technology (Italy), Erasmus Program, 1999.

[20] F.J. Molina, C. Alonso, C. Andrade, Cover cracking as a function of rebar corrosion: part 2-numerical model, *Mater. Constr.* 26 (1993) 532–548.

[21] K.Z. Hanjari, P. Kettil, K. Lundgren, Analysis of mechanical behavior of corroded reinforced concrete structures, *ACI Struct. J.* 108 (2011) 532–541.

[22] ACI 318-14 A, Building code requirements for structural concrete (ACI 318-14) and commentary, American concrete Institute, Farmington Hills, Mich, 2014.

[23] Du Y.G., Clark L.A., Chan A.H.C. “Effect of Corrosion on Ductility of Reinforcing Bars”, 2005, *Magazine of Concrete Research*, 57(7), 407-419.

[24] Design of concrete structures: CEB-FIP Model-Code 1990, London, UK, 1990.

[25] D. Coronelli, P. Gambarova, Structural assessment of corroded reinforced concrete beams: modeling guidelines, *J. Struct. Eng.* 130 (2004) 1214–1224.

[26] T.E. Maaddawy, K. Soudki, T. Topper, Analytical model to predict nonlinear flexural behavior of corroded reinforced concrete beams, *ACI Struct. J.* 102 (2005) 550–559.



ISSN: 2277-3754

ISO 9001:2008 Certified

International Journal of Engineering and Innovative Technology (IJET)

Volume 7, Issue 3, September 2017

AUTHOR'S PROFILE

Mohamed Mahmoud Husain "Prof. of Structural Eng., Faculty of Engineering, Zagazig University".

Heba A. Mohamed "Associate Prof., Department of Structural Eng., Faculty of Engineering, Zagazig University".

Sayed Ahmed "assistant Lecturer, Department of Structural Eng., Faculty of Engineering, Zagazig University".